Econ. Environ. Geol.
Vol. 31, No. 2, p. 127-139, 1998.

3-D Crustal Velocity Tomography in the Southern Part of The Korean Peninsula

So Gu Kim* and Qinghe Li**

ABSTRACT : A new technique of simultaneous inversion for 3-D seismic velocity structure by using direct, reflected, and refracted waves is applied to the southeast part of the Korean Peninsula including Pohang Basin, Kyongsang Basin and Ryongnam Massif. Pg, Sg, PmP, SmS, Pn, and Sn arrival times of 44 events with 554 seismic rays are inverted for locations and crustal structure. 6×6 with 0.5° and 8 layers (4 km each layer) model was inverted. 3-D seismic crustal velocity tomography including eight sections from surface to Moho, ten profiles along latitude and longitude are analyzed. The results are as follows: 1) the average velocity and thickness of sediment are 5.04 km/s and 3-4 km, and the velocity of basement is 6.11 km/s. The shape of velocity in shallower layer is agreement with Bouguer gravity anomaly (Cho *et al.*, 1997). 2) the velocities fluctuate strongly in the upper crust. The velocity distribution of the lower crust under Conrad appears basically horizontal. 3) the average depth of Moho is 30.4 km, and velocity is 8.01 km/s. 4) from the velocity and depth of the sediment, the thickness, velocity and form of the upper crust, and the depth and form of Moho, we can find the obvious differences among Ryongnam Massif, Kyongsang Basin and Pohang Basin. 5) the deep faults (a Ulsan series faults) near Kyongju and Pohang areas can be found to be normal and/or thrust faults with detachment extended to the bottom of the upper crust.

INTRODUCTION

The tomographic inversion of local seismic travel time data has been become a very efficient technique to study the earth's 3-D crustal structure with ever-increasing availability of more powerful computers and higher quality of seismic data. Many scientists have studied the seismic inversion methods (Aki, Lee, 1976; Backus, Gilbert, 1967; Benz, Smith, 1984; Crosson, 1976; Hawley *et al.*, 1981; Koch. 1985a, b, 1993; Lees, Crosson, 1989; Liu, 1984; Sambridge, 1990; Tarantola, 1987, 1992; Thomson, Gubbins, 1982; Thurber, 1983, 1985; Walck, Clayton, 1987).

The major problem of seismic tomography inversion is the multi-solutions. The coupling phenomena between hypocentres and seismic velocities make the seismic tomography from the relative results of velocity and hypocentre. One of procedure is decoupling of hypocentres from the structure which reduce the dimensions of the matrix of the Frechet derivative significantly, or the use of subspace method. The uses of linear equations to non-linear inversion make bias distortion of the result from practice. However, in case when the initial model is well chosen and is sufficiently close to the true minimum of the objective function, a linear or at least a quasi-linear treatment appears to be vindicated. The ill posed of the seismic inversion which induced by the trade-off between hypocentres and seismic velocities is most complex. Whereas the concept of regularization is fairly well understood for linear inversion, one has to use a general theory for the non-linear inversion (Koch, 1993).

The increasing of independent parameters to attend inversion is key for physical meaning. As we know, it is not increasing the amount of data (of course, the co-linear data have to be need), but if the independent data which possess common physical base as constrained condition participates in inversion, may be these data can help to solve the puzzled of pure mathematical algorithm.

In this paper, we introduce the seismic inversion basic principle, constrained inversion methods, including P and S wave simultaneous inversion, combining DSS (deep-seismic sounding) and earthquake data, optimal regularization and error estimation. Pg, Sg, PmP, SmS, Pn, and Sn are common phases understood by the most seismologists. The relative seismic phases have similar seismic ray paths, so they can mirror the same interface. We can inverse the phase readings simultaneously by using them as constrained condition to reduce multi-solution of results. Because the rays of Pg, PmP, and Pn propagate through different parts of crust, so combining them can get the information from top to bottom of the crust. According to above me-

* The Seismological Institute, Hanyang University, Ansan 425-791, Korea
** Lanzhou Seismological Institute, SSB, Lanzhou, 730000, China

thods, the computer program "3DZL" was performed.

The Korean Peninsula is located near the boundary of the Pacific plate and the Eurasian plate. In the view of plate motion, this peninsula is a transition zone of two plates. The deep structure can reflect the induction and deduction of plate motion. But up to now, there is a blank for 3-D seismic velocity distribution. The area of southeast of Korea Peninsula is a tectonic active region. The Kyongsan Basin, the Pohang Basin and the Ryongnam Massif play important rolls in tectonic research. We give the 3-D seismic inversion tomographic results including 8 sections from surface to Moho, 10 profiles along latitude and longitude respectively, and Moho depth distribution. According to these images, we analyzed the structural characteristics of sedimentary, basement, the upper crust, Conrad, the lower crust and the Moho. The deep fault features were investigated, and the major difference of deep structure for different geological province was studied.

METHODOLOGY

Basic principle

The general expression for the seismic traveltime T_{ij} between ith (i=1, 2, $\cdots m_e$) event and jth (j=1, 2, $\cdots n_s$) station is:

$$T_{ij} = \int_{L_{ij}} u(r)\, ds \tag{1}$$

where is position vector, u(r)=1/v(r) is wave slowness, v(r) is velocity vector, L_{ij} is ray pass between hypocentre and station, and ds is ray element.

The traveltime T is a non-linear function of velocity v. Using Fermat's principle, the first correction of traveltime is induced by the perturbation of wave slowness, as well as the unknown source. So the perturbation equation can be written as (Liu, 1984):

$$\delta T_{ij} = \int_{L_{ij}} \delta u ds + \delta x_{iq} \cdot \nabla_{x_i} T_{ij} \tag{2}$$

where (q=1, 2, 3, 4) are latitude, longitude, depth and original time of source.

For m_e events and n_s parameters of waveslowness:

$$t = cy \qquad c = (A, B) \qquad y = (\delta v^T, \delta x^T)^T \tag{3}$$

where t is traveltime vector, c is coefficient matrix, and y is a solve vector including source parameter δx and model parameters δv.

$$\begin{aligned} t &= (t_1, t_2, \cdots t_{m_e})^T \\ A &= (A^1, A^2, \cdots A^{m_e})^T \\ B &= \mathrm{diag}(B^1, B^2, \cdots B^{m_e})^T \end{aligned} \tag{4}$$

$$A_{ij} = \int_{L_{ij}} \frac{\partial u}{\partial v_q} ds \tag{5}$$

$$B_{ij} = \frac{\partial T_{ij}}{\partial x_{ik}};$$

$$\begin{aligned} l &= n_e(i-1)+j \\ q &= 4(i-1)+k \end{aligned} \tag{6}$$

where $m=m_e \times n_s$, A is $m \times n$ matrix, B is $m \times 4m_e$ matrix, t is the residual time vector of m dimensions, if $t_{ij}^{(0)}$ is observational arrival time, and O_i is "guess" original time, then:

$$\begin{aligned} t_i &= t_{ij}^{(0)} - O_i - T_{ij}, \\ l &= n_2(i-1)+j \end{aligned} \tag{7}$$

$$\begin{aligned} \delta x &= (\delta x_1, \delta x_2, \cdots \delta x_{m_e})^T \\ \nu x &= (\delta \nu_1, \delta \nu_2, \cdots \delta \nu_{m_e})^T \end{aligned} \tag{8}$$

Under non-constrained condition, the solution vector of equation (3) can be indicated as minimum norm:

$$\| t - cy \|_2^2 = m \tag{10}$$

The formula (9) is equivalent to minimum norm solution δv.

If the orthogonal projection operator of image space $\Gamma(b)$ in which ω^m project to B, B^+ is general Moore-Penrose inverse matrix of B, was writeen as : $P_B=BB^+$, then (9) can be rewriteen as:

$$\begin{aligned} &\| t - cy \|_2^2 = \\ &\| P_B(t-cy) \|_2^2 + \| (I-P_B)(t-cy) \|_2^2 = \min \end{aligned} \tag{10}$$

where I is unit matrix, insert (3) to (10), then

$$\begin{aligned} &\| t - cy \|_2^2 = \\ &\| P_B(t - A\delta v) - B\delta x \|_2^2 + \\ &\| (I-P_B)t - (t-P_B)A\delta v \|_2^2 = \min \end{aligned} \tag{11}$$

(11) is equivalent to minimum norm solution $\delta\hat{v}$ and $\delta\hat{x}$ respectively:

$$\| (I-P_B)t - (I-P_B)A\delta\hat{v} \|_2^2 = \min \tag{11a}$$

$$\| P_B(t - A\delta\hat{v}) - B\delta\hat{x} \|_2^2 = \min \tag{11b}$$

After some calculating, we can get the model estimation of and respectively.

Constrained inversion

A. P and S simultaneous inversion

We know that the earthquake source can emit P and S wave spread for the spherical surface. Since the P and S waves can reflect the same interface, we can inverse them simultaneously as constrained conditions to reduce multi-solution of inversion. Because Pg and Pn phases can be distinguished easily as the first arrivals in various distances, the amplitude of PmP is stronger in suitable distance, so Pg, Pn, PmP and corresponding Sg, Sn, SmS are common phases understood by most seismologists. The rays of Pg, PmP, and Pn propagate through different parts of crust, so the combining of them can get the information from top to the bottom of the crust, especially the seismic rays from PmP and Pn can thread upgoing to the upper crust, so the information density in the upper crust is investigated.

We are also interested in detecting the behind deep faults due to the anisotropy of high fluid pressure in the upper crust. In this study we use Pg, Sg, PmP, SmS, Pn, and Sn to inverse whole crust for increasing the constrained condition for inversion.

B. Combining the DSS data and earthquake data to simultaneously inverse

Having DSS data, accuracy location, original time and dense stations on line the reliability of the seismic tomography is increased, since the accuracy of result of DSS is higher than earthquakes.

Assume there are m_1 explosions and m_2 earthquakes, then equation (11) can be rewriteen as (Li *et al.*, 1994):

$$\| P_1 - P_2 \|_2^2 = \min \tag{12}$$

$$P_1 = \begin{bmatrix} t_{m_1} \\ (I - P_B)t_{m_2} \end{bmatrix} \qquad P_2 = \begin{bmatrix} A_{m_1} \\ (I - P_B)A_{m_2} \end{bmatrix} \tag{13}$$

If we set velocity constrain for 2-D velocity structure from DSS, then (12), (13) can be rewritten as:

$$\| P_3 - P_4 \|_2^2 = \min \tag{14}$$

$$P_3 = \begin{bmatrix} v_{m_1} \\ (I - P_B)t_{m_2} \end{bmatrix} \qquad P_2 = \begin{bmatrix} A_{m_1} \\ (I - P_B)A_{m_2} \end{bmatrix} \tag{15}$$

where v_{m_1} denotes velocity known.

If there are several DSS lines across on same area, we can construct them as a fixed model to use above formulae (12-15).

Optimal regularization

We select Leveaberg-Marquardt method to get the optimal regularization. It is demonstrated that the LM method, in spite of its computational inexpediences has various properties that make it best suited for the solution of both the general non-linear inverse problem and its linearized subproblems. (Koch, 1993).

Database

We constructed database to get the results of profiles to analyze the velocity distribution as depth directly.

Error estimation

Following equations are used for estimating resolution and error.

a) The resolution of the model is computed from the resolution matrix:

$$R = (B^T B + kI)^{-1} B^T B \tag{16}$$

b) The covariance of solution is:

$$\mathrm{cov}(\delta v) = (B^T B + kI)^{-1} R\sigma^2 \tag{17}$$

In (16) and (17), R is resolution matrix, B is Jacobian matrix and B=∇T, B^T is a transposed matrix of B, I is unit matrix, δv is model vector, and σ^2 is the variance of the data which is either estimated a priori or is evaluated from the a posteriori residual sum squared.

GEOLOGICAL BACKGROUND OF RESEARCH AREA

Cho *et al.* (1997) introduce briefly the geological background of southern part of the Korean Peninsula. The Korean peninsula constitutes in general, the eastern part of the Sino-Korean Paraplatform. The southern part of the Korean Peninsula is composed of NE-SW trending geologic provinces. They are from the northwest to southeast, a) the Precambrian Kyonggi Massif consisting of gneisses and schists, b) the Ogcheon Fold Belt with Paleozoic and Mesozoic marine and non-marine strata, c) the Precambrian Ryongnam Massif composed of gneisses and schists, d) the Cretaceous non-marine Kyongsang Basin and the Neogene Pohang Basin. Besides, the volcanic province of Quaternary age, Cheju island, is situated off the south coast.

Southern Korea comprises most of tectonic provinces arranged in NE-SW direction: the Cretaceous Kyongsang Basin, the Precambrian Ryongnam massif, the Ogcheon Fold Belt and the Precambrian Kyonggi massif from southeast to northwest. The massifs are basement complexes consisting largely of gneisses and

subordinately Jurassic granite. The Late Triassic Songrim Disturance and the Jurassic Daebo orogeny, which was accompanied by strong plutonism and volcanism played important roles in structural deformation and metamorphism of pre-existing rocks.

In the Korean Peninsula three tectonic alignments are prominent and well expressed by its topography. The alignment direction is the one that trends N-NW and is represented by the Taebaek Mountains, which runs parallel to the east coast in South Korea. The alignment direction in south Korea probably originated from a tilting along faults close to the shore in the east Sea. The titling has created the topographic characteristics of the peninsula, which is characterized as a whole by mountainous regions in the east and lowlands in the west. Therefore we can see major direction of alignments NE-SW in inland and NW-SE near the coastal areas of the southeastern parts of Korea.

The Sinian direction is represented by a NE-SW direction which is mainifested by the trend of the Okcheon Zone and a distribution pattern of the Daebo granite batholith of the Jurrasic to Early Createceous. In the southern part of Korean Peninsula the direction is well expressed by a few mountain ranges such as Kwangju, Charyong, Sobaek, Noryong and Togyu ranges from north to south.

The Ryongnam Massif is situated in the southern part of Korean Peninsula bounded by a fault with the Okchon Folded Belt on the northwest and with the Kyongsang Basin. The Fig. 1 illustrates stations, events, and seismic rays in our research.

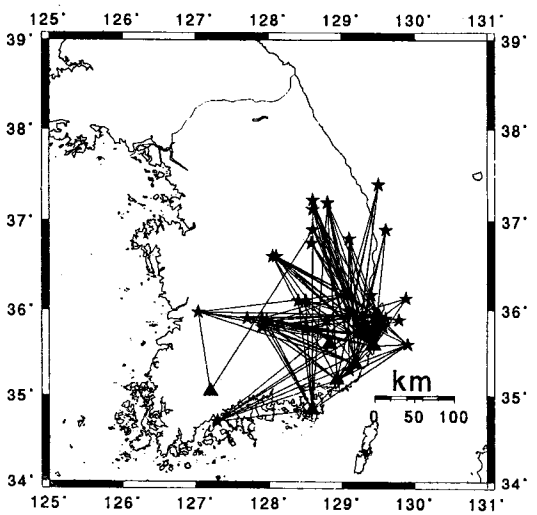

Fig. 1. The seismic ray paths for the southeastern part of South Korea Triangles and stars indicate stations and events, respectively.

DATA PROCESSING

Data

There are 10 seismic digital stations installed by KIGAM around research area, Table 1 illustrate the stations parameters.

The data used in research area are local arrival times of 44 earthquakes occurring between December 1995 and December 1996. The local magnitude (M_L) of the earthquakes range between $1.6<M_L<3.3$. Depending on their sizes, events have been recorded at 3-8 stations. The epicentral parameters were relocated by using KMA bulletins, KIGAM reports, HYPO71PC, and single station 3-comp. method (Kim and Gao, 1997).

We analyze three seismic phases to inverse velocity structure and relocation.

a) Pg the epicentral range of 20~120 km as the first arrival pickings, and they are direct waves, almost they emitted upgoing from source to stations. Because these phases are tip and clear, so the accuracy of them is higher and can reach 0.1~0.2s.

b) PmP the reflection waves from the Moho, and the epicentral range of 90~250 km to use, including overcritical distance. This phase has stronger amplitude even thought it is as a later arrival phase after some wavelet. The accuracy of picking up can reach about 0.2s.

c). Pn the refraction waves along the Moho. From 160 km it can emerge as the first onset but amplitude is small. They are clearer and tip with increasing epicentral distance and the duration time between Pn and PmP are longer. However, because the energy from Pn is not stronger, so the onset is not clear on some distance, and the accuracy is not higher. We think the accuracy can reach about 0.2s.

d). S-wave including Sg, SmS, and Sn corresponding to Pg, PmP and Pn. They are later phase, so determining the arrival is difficult and the error will

Table 1. Station parameters.

No	Station	Latitude			Longitude			Height
		D	M	S	D	M	S	km
19	BBK	35	34	48	129	26	24	0.2
20	CHS	36	10	48	129	05	24	0.2
21	DKJ	35	56	24	129	06	36	0.2
22	HAK	35	55	48	129	30	00	0.2
23	KJM	34	49	48	128	35	24	0.2
24	KMH	35	10	48	128	55	48	0.2
25	MAK	35	22	12	129	10	48	0.2
26	MKL	35	43	12	129	14	24	0.2
27	GRE	35	03	00	127	12	00	0.2
32	CGD	35	36	00	128	49	59	0.2

be larger, and we think the accuracy will be about 0.2~0.3s.

The hypocentres are subjected to certain quality criteria. Thus the following events are eliminated from the inversion if: (1) they occur outside the area of the model (2) the quality of the hypocentre location attributed by HYPO71 is poor in case of fewer than three stations recorded. These criteria reduce the original events, finally we select the data to inverse as 44 events with 153 for Pg and Sg, 91 for PmP and SmS, and 33 for Pn and Sn in the research area.

Mode and Initial model

We select plane layer block model with discrete velocity parameters. For this model, each horizontal layer is divided into blocks of equal size. A constant velocity is defined at each block. Within each layer and among different layer the interpolating function was used. This makes the model applicable to 3-D ray tracing techniques. Fig. 2 shows map of study area and seismic profile lines (B-B', C-C', M-M', and N-N').

According to the data and geometry of research area, we determine inversion mode as:

Scope: 34.5°~37.5°N, 127°~130°E

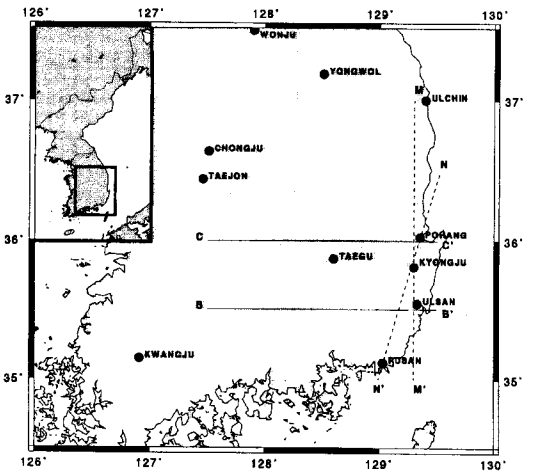

Fig. 2. The seismic cross section map. The seismic profiles of B-B', C-C', M-M', and N-N' are given in Fig. 4.

Block: 6×6 with 0.5° (44.2×55.3) km

Layers: 8 layer with 4 km each layer.

According to former research results (Kim & Kim, 1983, Kim & Jung, 1985, Kim & Lee, 1994), we try to calculate several tens models to test the stability of various models. After comparing them we determine the initial model shows as Table 2.

Inversion processing

We had experiments to test the suitable model. The test results demonstrate that for various models, the Moho form and the velocity distribution are similar basically. It means that the inversion method is independent of the initial model, and the result is stable. Of course, the model result is close to actual practical situation.

Optimal solutions will then be retrieved using the various optimal regularization techniques, lengthy objective and subjective evaluations of these models and of some personal judgement based on the practical experience of the author. The trade-off characteristics for regularization and resolution have to be performed.

In addition, optimal solutions are also eventually based on the minimization criteria for the non-linear objective function, or the total residual sum. The RMS value of the traveltime residuals obtained for most of the seismic events lie in the range 0.1~0.2s. The standard deviations for the epicentral coordinates are 2 km and for the depth is 5 km. In our computer program, we have a termination criterion for the iteration. The final result is comfortable for the above.

We got 8 isovelocity tomography cross sections corresponding to the stratified model (See Figs. 3a and 3b). The Moho distribution was also obtained (See Fig. 4). According to our main interests, we construct 4 seismic profiles along latitude and longitude. These images are shown on Fig. 5. The confidences of results in four corners are less because the rare seismic rays pass through that area.

Fig. 3a and 3b show the tomographic sections from surface to Moho. Fig. 4 is the Moho distribution. The inversion scope and profiles are shown in Fig. 4. Fig. 6 also shows the velocity model obtained from receiver function (Lee, 1997). The Moho depth is estimated is as 28.0 km from this analysis.

Table 2. Initial model.

Layer	1	2	3	4	5	6	7	8
Depth (km)	0-4	4~8	8~12	12~16	16~20	29~24	24~28	28~32
Velocity (km/s)	5.00	6.18	6.35	6.45	6.65	6.90	7.40	8.05

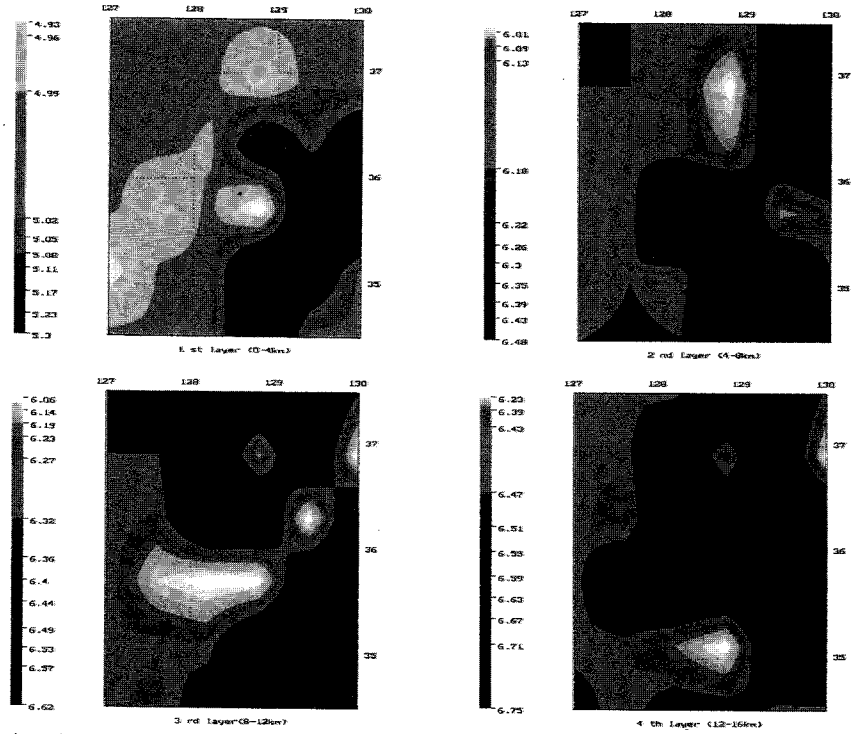

Fig. 3a. The isovelocity map along the horizontal plane. Each block thickness is 4 km including 1st through 4th layer. We can see the high velocity at 3~4 km and low velocity at 1 km near Pohang area.

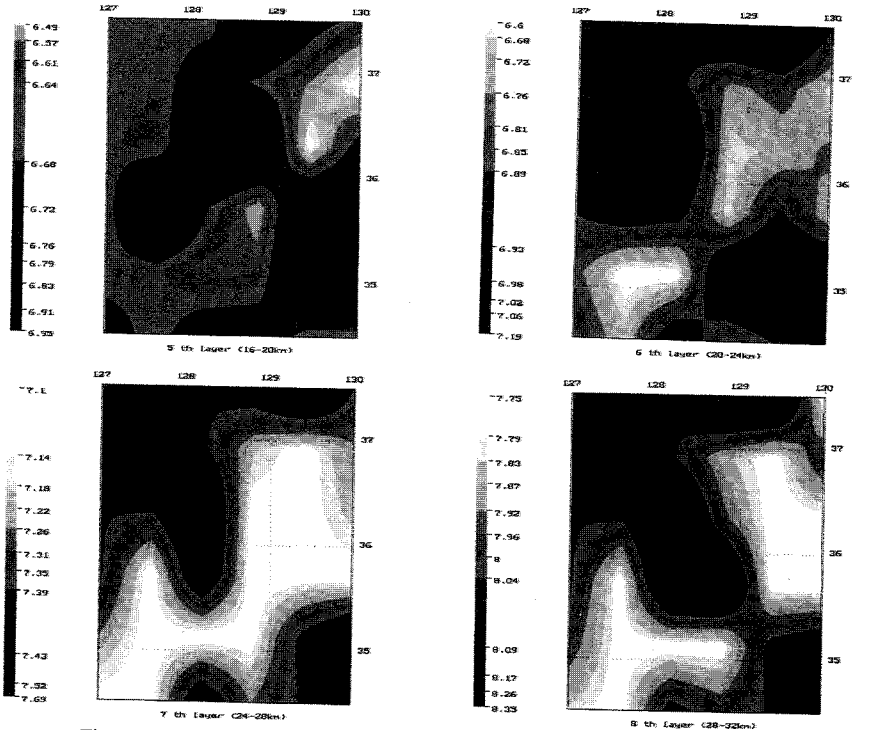

Fig. 3b. The same as Fig. 3a but from 4th through 8th layer. We can see the low velocity layer at the lower crust.

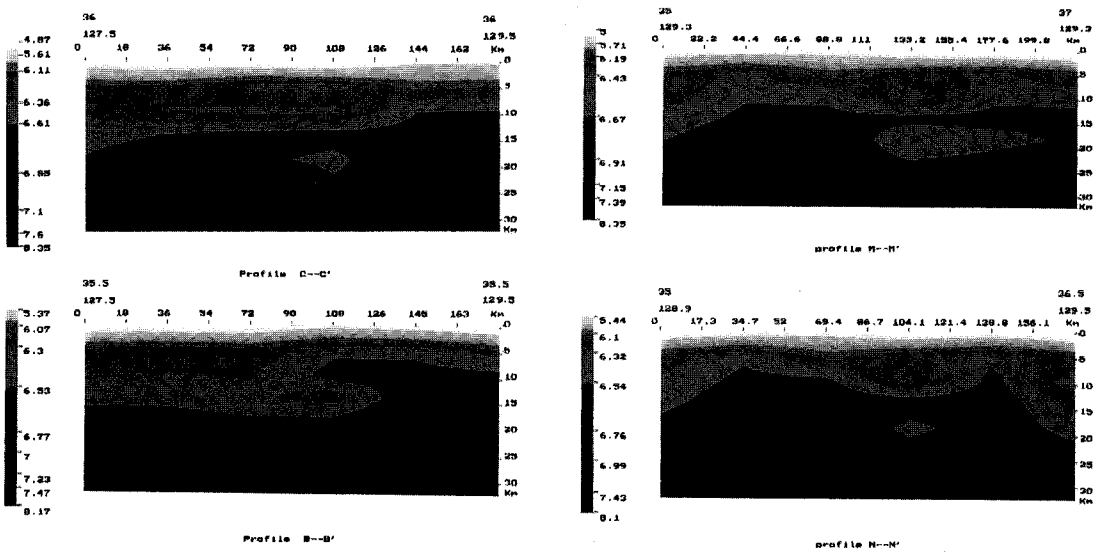

Fig. 4. The cross sections of the seismic profiles along the vertical planes. We can see the velocity anomalies near Pohang, Kyongju, and Ulsan areas from the seismic profiles, B-B', C-C', M-M' and N-N'.

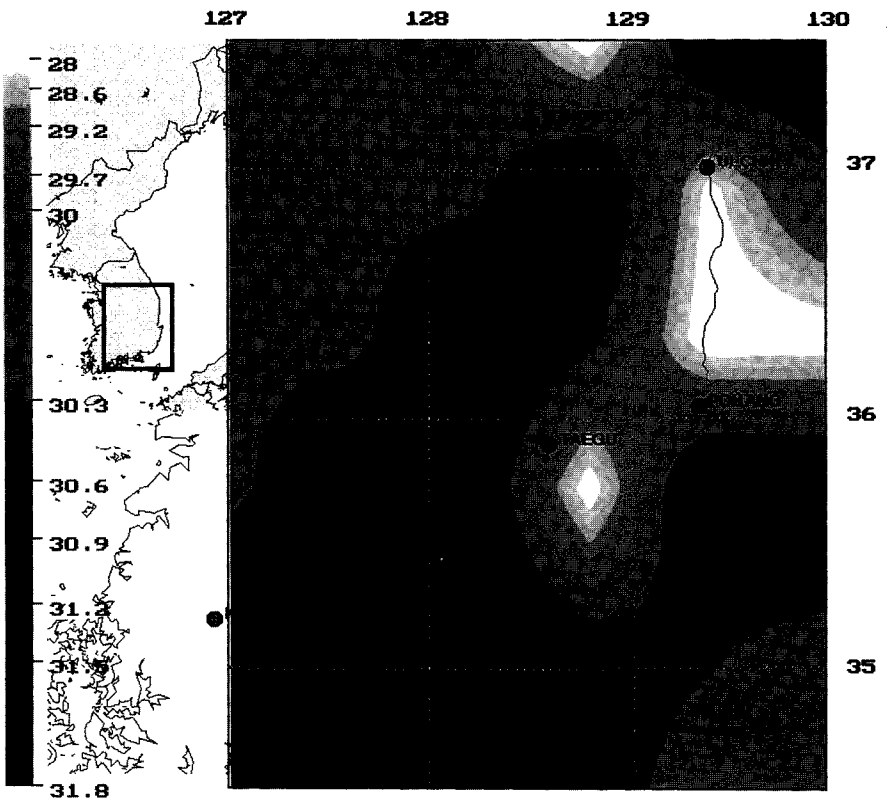

Fig. 5. The contour map of the crustal thickness under the southeastern part of South Korea from 3-D seismic tomography. The Crustal thickness are determined as 30.7 and 29.5 km mear the Kyongsang and Pohang basins, respectively.

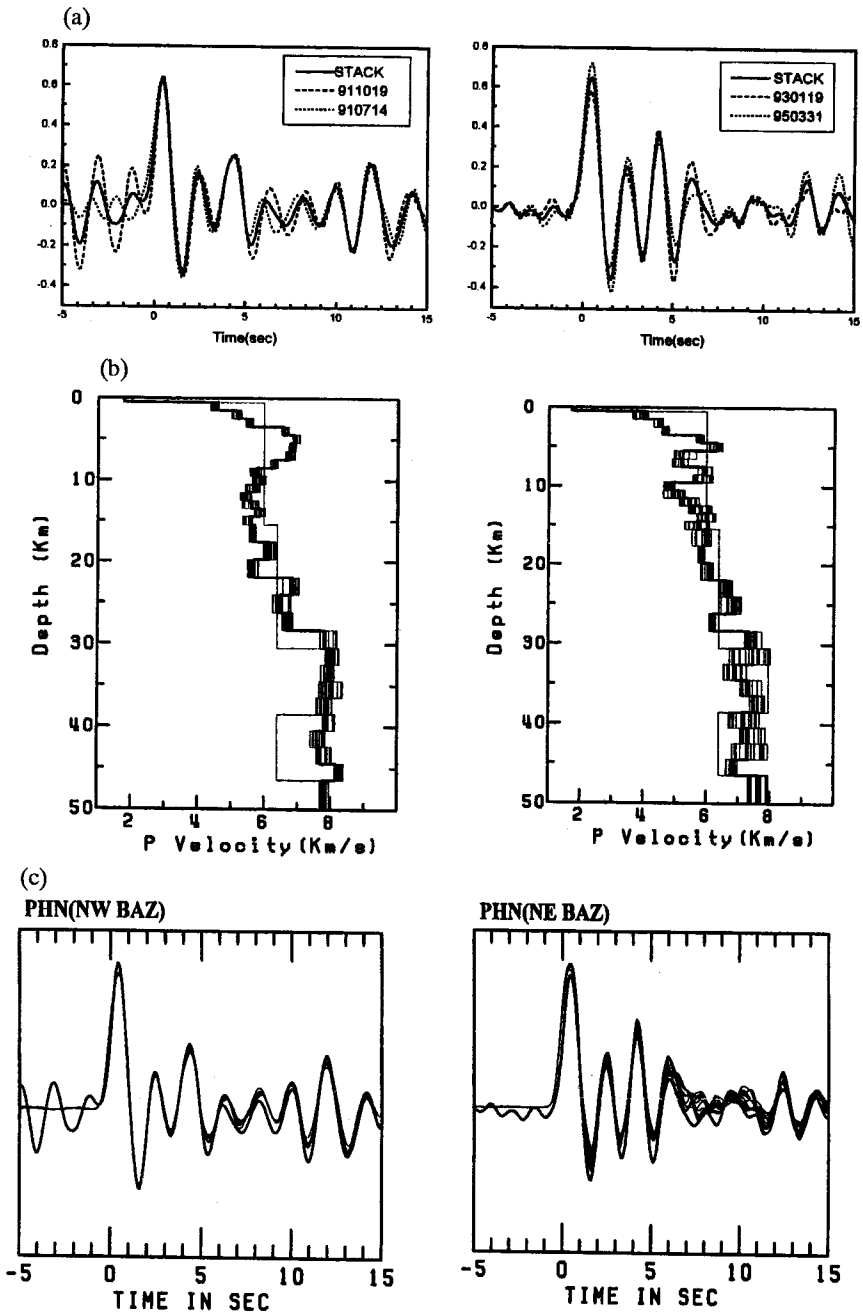

Fig. 6. Inversion of receiver functions for the Pohang station (PHN). a) individual (dashed, dotted) and stacked (solid) receiver functions for NW direction for teleseismic events and NE direction for deep-focus events. b) final (thick solid) and initial (thin dotted) velocity models for the Pohang station. c) receiver function waveform fits, thick and thin solid lines indicate stacked and synthetic receiver functions, respectively (Lee, 1997).

MAJOR RESULTS

Sedimentary Layer and Basement

Combining the profiles and horizontal sections (see Fig. 3a, 3b, 4, and 5), we can get the information for basement and sedimentary layer as follows:

The average velocity in sedimentary rock is 5.04 km/s in general, in some region it can reach 5.5 km/s. The depositing thickness of sediments are about 3-4 km in general, but for various regions they are not the same, and deepest is 6 km in some area, and it appears shallower (about 2-3 km). The sedimentary layer has 4-5 velocities strata, they are 4.8, 5.4, 5.6, 5.8, 6.0 km/s respectively. The area contoured by 35.5°~37.5°N, 128°~129°E except the northeast and southwest corner represents deeper depositing, especially following areas: a) 35.5°~36.2°N, 128.7°-129.5°E (about Kyongju, Yongchon, near Pohang), it is Pohang Basin; b) 36.4 (-N, 127.8 (-128.7 (E (about Sangju, Chungju), it is a part of Kyongsang Basin. We can see a velocity model of Pohang station using receiver functions from Fig. 6 (Lee, 1997). We can see the rapid velocity gradient at about 3~5 km and the low velocity layer at about 10 km deep and the Moho depth is estimated as 28 km.

The average basement velocity is 6.11 km/s, and highest is 6.18 km/s and lowest is 6.02 km/s.

a) In the Bouguer anomaly map, there is a triangle-shape region, i.e. contoured by (37°N, 129.2°E), (35°N, 127.7°E) and (35.2°N, 129.4°E), the higher Bouguer anomaly (10~65 mgal) exist, and we can see also that in (36.8°N, 130.0°E), (34.5°N, 128.2°E), (34.7°N, 129.7°E), the velocities are higher.

b) In the northwest of a line linked between two points (37°N, 129.0°E) and (34.3°N, 126.8°E), there are lower Bouguer anomaly (-45-0 mgal). On the same site the velocities are lower.

c) In a small area (35.5°~36°N, 128.5°~129.0°E), there are lower velocities and lower Bouguer anomaly, especially, the position with lowest velocity is coincident lowest Bouguer in the same area.

d) A small area with higher velocity (36°~36.5°N, 128.5°~129°E, v=5.08~5.17 km/s) has higher Bouguer anomaly (10 mgal).

e) There are two lowest Bouguer anomalies regions with 10~20 mgal, in the same area, the velocities are lower with 4.93~4.99 km/s.

Conrad discontinuity

In the result of research tomography, there is a velocity discontinuous layer that is divided into the upper and the lower. The characteristics of isovelocity contour in the two parts are remarkably different. This interface is Conrad discontinuity. In the upper crust, the velocity distribution form fluctuate obviously, some higher (lower) velocity layer (body) embed in normal layer. But in the lower crust, horizontal velocity layer can be displayed.

The average velocity on Conrad layer is about 7.06 km/s, the highest is 7.14 km/s, and the lowest is 6.92 km/s. The average depth of Conrad is 21.2 km with 26.1 km deepest and 14.5km most shallow.

The moho discontinuity

Fig. 5 is the Moho depth distribution. The average depth and velocity of Moho in research area is 30.4 km and 8.01 km/s with 8.07 km/s (highest) and 7.92 km/s (lowest) respectively. The form represents deeper in west and shallower in east. There are three small areas with shallower depths: a) 35.3°~36°N, 128.5°~129.2°E (around Taegu), the depths are about 28-30km; b) 36°~37.2°N, 129°~130°E (around Andong, Yongdok, Pohang), about 28~30 km; c) 37.3°~37.5°N, 128.4°~129°E, with 28~30 km. Deeper Moho areas are: a) 35.3°~36°N, 129.2°~130°E (around Kyongju, Ulsan), about 30~31.5 km; b) west of 129(E except above shallower area, it is about 30~31.8 km, the deepest is 34.5°~35.5°N, 127°~128.3°E (around Sunchon), about 31.8 km.

We found that in the Ryongnam Massif the Moho is deeper, in Kyongsang Basin and Pohang Basin the Moho is shallower. It is an essential feature of this area.

Major characteristics of the upper crust

The crust of research area can be divided into the upper and the lower parts. The interface is Conrad. From surface to 20~21 km is the upper crust. The upper crust has four velocity layers except for the sedimentary layer.

For the first layer under basement, the average velocity is 6.11 km/s, and the scope variations are 6.02~6.18 km/s. This layer presents horizontal basically and the thickness is 1.5~2.5 km in general, and most thick is 5 km and shallow is 1km.

The average velocity of the second layer is 6.35 km/s and the highest is 6.42 km/s, and the lowest is 6.25 km/s. The thickness of isovelocity changes from 1 km to 13 km, appearing stronger inhomogeneity.

The average velocity of the third layer is 6.58 km/s and the highest is 6.66 km/s, and the lowest is 6.47 km/s. The thickness variegates from 2 km to 15.2 km.

The average velocity of the fourth layer is 6.82 km/s, the highest is 6.90 km/s and the lowest is 6.70 km/s. The thickness variegates from 2 km to 15.6 km, the inhomogeneity can be found.

A remarkable boundary line among higher and lower area is coincident with different geological province. On the profiles scope, the Ryongnam Massif, Kyongsang Basin and Pohang Basin present higher area, lower area (including small higher area) and higher area respectively, the outline shows the

boundary line for various geological provinces.

The major characteristics of the lower crust

A remarkable feature of the lower crust is that the form of the lower crust appears horizontal basically. The depth from 21.2 km to Moho (30.4 km) is the depth scope of the lower crust. There are three velocities layer in the lower crust. i.e., the first layer has average velocity of 7.06 km/s with 4.3 km thickness, and it is Conrad layer. The second layer has average velocity of 7.32 km/s with 2.7 km thickness. The third layer has average velocity of 7.61 km/s with 2.2 km thickness.

The stronger inhomogeneous upper crustal velocities and horizontal stratified lower crust may indicate that the tectonic movement happened mainly in the upper crust. In contradiction to some area of inter-plate or intra-continent where the Moho and the lower crust has stronger inhomogeneity, the different lower crust form may reflect that the tectonics and movement manner, evolution and geodynamics in this area are not similar to above area.

For the kyongsang basin and pohang basin

The tectonic situation

Kyongsang Basin was formed in front of the Ryongnam Massif after the fading of the Daebo Orogeny. It extended to the western Japan which was located close to Asian Continent during the Cretaceous to Early tertiary before drifting to the southeast of its present position. The Kyongsang Basin is a broad downwarpring basin, rising slightly in the east near the present southeastern coastal area.

The Cretaceous sediments in the basin exhibit a kind of molasse type consisting of conglomerate, sandstone, shale and some pyroclastics. The sediments have been differentiated into the so-called Nagtong, Silla and Bulguksa Series in ascending order. As to the depositional environment there are wide ranges of opinion, such as floodplain and lacustrine.

Due to pre-existing topography prior to the sedimentation, the basin is subdivided into the Yongyang, Uisong and Kyongsang proper subbasins from the northeast to the southwest. The sedimentary formations in the basin dip generally southeast showing homoclinal nature, thought broad open folds exist in many places. At the close of Cretaceous intermediate volcanic rocks extruded onto the basin covering the southcentral part of the basin forming the Yuchon Group. Subsequent to th volcanic activity with age ranging from Late Cretaceous to Early Tertiary.

Trends of faults in the basin area show predominantly a north-northeast direction with subordinate west-northwest and east-northeast tendencies. Plate tectonic movement affected the Kyongsang Basin from the Late Cretaceous to Tertiary as the Japanese Islands drifted southeastward from the Asian Continent.

The Pohang Basin is composed of terrestrial sediments at the lower horizons and marine sediments at the upper horizons. Both of them belong to the Miocene, but the later rests unconformably on the former. These formations show a monotonous structure striking north-northeast and dipping east with minor open fold in this places (Kim, 1982).

The feature of sediment and basement

There is a obvious shallower boundary line between Kyongsang Basin and Ryongnam Massif on the shallower layer, see first layer section (Fig. 3a). From Fig. 4 and 5 we can calculate the velocity distribution and buried depth form. In general, the average velocity in shallower layer (0~4 km) of the Kyongsang Basin is 5.06 km/s except a small area, higher than the Ryongnam Massif (4.98 km/s). The small area is near Taegu, has lower velocities, about 4.93~4.99 km/s. The lower velocities area is coincident with lower Bouguer anomaly area (0~10 mgal) (Cho *et al.*, 1997). The buried sedimentary depth of Kyongsang Basin are 3~4.2 km. In the Ryongnam Massif, h=2.5~4 km. The velocity of basement in the Kyongsang basin is 6.07~6.18 km/s.

The buried sedimentary depth of Pohang Basin is 3~4.5 km, and average velocity is 5.15 km/s, it is higher than Kyongsang Basin and the thickness of deposit is more than later. The velocity of basement is 6.11~6.18 km/s for Pohang Basin.

The feature of upper crust

From the Fig. 4, we can find the features of the upper crust among Ryongnam Massif, Kyongsang Basin and Pohang Basin are very different.

In the Pohang Basin, the velocities of the upper crust are higher, that is, the form of velocity ascends. In the Kyongsang Basin, the velocities of the upper crust are lower, that is, the form of velocity descends (See Figs. 3a and 3b). In the primary impression from the rough data in the Ryongnam Massif, the velocities also ascend.

The moho form

The Moho depths are 29.5km for Pohang Basin, 30.7 km Kyongsang Basin and 31.1 km for Ryongnam Massif respectively.

General impression

For Pohang Basin, Kyongsang Basin and Ryong-

Table 3. Major features of various provinces.

		Ryongnam Massif	Kyongsang Basin	Pohang Basin
Sediment	Thickness (km)	2.5~4	3.42	3-4.5
	Velocity (km/s)	4.98	5.06	5.15
Basement	Velocity (km/s)	6.02~6.18	6.07~6.18	6.11~6.18
Upper crust	Velocity (km/s)	Higher	Lower	Higher
Moho	Depth (km)	31.1	30.7	29.5
		Deep	Middle	Shallow

nam Massif, the velocity of sediment are higher, middle and higher, the thick of depositing are deep, middle and shallow, the velocities of the upper crust are higher, lower and higher, the Moho are shallow, middle and deep in order. The comparisons of major features are list in Table 3.

There are not only obvious difference between massif and basin, but also the Kyongsang Basin and Pohang Basin. They are different kinds of basin, and may be they have different creating and formatting mechanism.

For deep faults

After comparing the Fig. 4 (B-B', C-C', M-M', and N-N'), we can find that in the upper crust there are some interesting phenomena.

From Fig. 4, C-C' profile, we can find under 144km the velocity both east and west are not the same, the difference is 0.24~0.25 km/s, and if it is a index of fault, then may be on the east uplift and west downwarpring, the end can reach 23~24 km under surface, the extension point on the land may be located among Kyongju, Yongchon, and Pohang.

From Fig. 4 B-B' profile, we can find similar results too, that is, the velocity both east and west are not the same, the difference is also about 0.24~0.25 km/s. The end of velocity difference line can extend to westwards along 7.23 km/s interface. The emergent point on the land will locate west of Ulsan, depart from 20~25 km.

If it can be interpreted as the deep representation of the Yangsan fault, then the fault may be a normal and/or thrust fault, the upcast side is in east and downcast in west, and its strike direction is NE-SW, at least from above three break points can line the direction and dip. We also can think that this fault has not extend to 37°N and 34.5°N.

The outcrop location of faults in B-B' and C-C' profiles corresponds to 108~145 km on the profile lines. It may reflect that there are series of faults near Kyongju and Ulsan areas. Especially the normal and/or thrust faults in the upper crust are found in the east side profiles near Kyongju and Pohang areas. We think the Ulsan faults are detachments on the bottom of the upper crust.

CONCLUSSON AND DISCUSSION

The crust is composed from the upper and the lower parts. The interface of the upper and the lower crust is Conrad discontinuity.

The average velocities in sedimentary rock are 5.04 km/s, and the thicknesses of sediment above basement are about 3~4 km in general, but for various regions they are not the same. The Pohang Basin and Kyongsang Basin have deeper sediments. The average basement velocity is 6.11 km/s.

In the upper crust, the velocity distribution form fluctuate obviously, some higher (lower) velocity layer (body) embed in the normal layer. A remarkable feature of lower crust is the form of lower crust appears horizontal basically. The depth from 21.2 km to Moho (30.4 km) is the depth scope of the lower crust.

The average velocity on Conrad layer is 7.06 km/s, and the average depth of Conrad is 21.2 km. The average depth and velocity of Moho is 30.4 km and 8.01 km/s. The form represents deeper in west (Ryongnam Massif) and shallower in east (Kyongsang Basin and Pohang Basin).

For Pohang Basin, Kyongsang Basin and Ryongnam Massif, the velocities of sediment are higher, middle and lower, the thicknesses of depositing are deep, middle and shallow, and the velocities of the upper crust are higher, lower and higher, the Moho are shallow, shallow and deep in order. We can draw the outline of Basin according to the velocity distribution of the upper crust. We can see a high velocity layer at 3 km and a low velocity zone at around 10 km in the Pohang basin. This well agrees with the results of receiver functions (to see Fig. 6). The discontinuities by gravity and magnetic anomalies at Pohang region are also found to be at 3~4 km and near 11 km, respectively (Cho *et al.*, 1997). The Yangsan and Ulsan

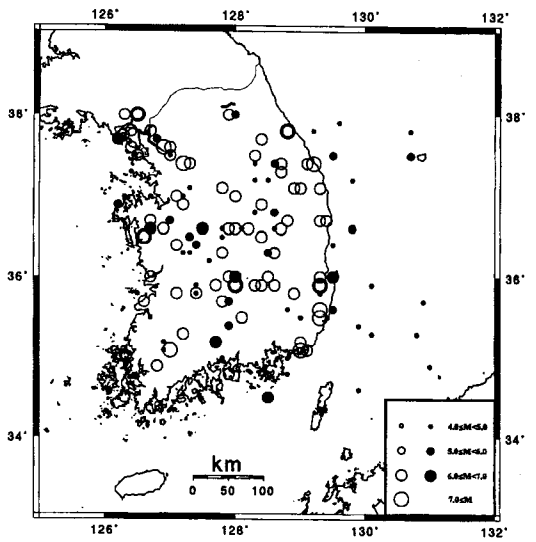

Fig. 7. The seismicity map of the South Korea. The open and closed circles indicate historical (A.D. 27~1905) and instrumental earthquakes (1906~1997), respectively.

Faults have deep displays from the profiles, and they may extent to the bottom of the upper crust as a detachment form. This is coincident with the earthquake occurrence near Kyongju and Ulsan areas in Fig. 7.

Due to lack of the events, the confidence of four corners of inversion scope is less reliable. We have to obtain more interpretation of geology and geophysics for anomalous velocity distribution in seismic tomography investigation. Besides we shall have more detailed and accurate 3-D tomography as higher quality data are retrieved as we expect in the very near future.

AKNOWLEDGEMENT

This work was supported by the Korean Research Foundation (1996) and STEPI. The second author is sincerely grateful to the Seismological Institute, Hanyang University during his stay as a visiting professor. Authors are also indebted to M.S. Bae for his computer work.

REFERENCES

Aki, K. and Lee, W.H. (1976) Determination of three dimensional velocity anomalies under a seismic array using first P arrival from local earthquakes 1. A homogeneous initial model. J. geophys. Res., v. 81, p. 4381-4399.

Backus, G.E. and Gilbert, F. (1967) Numerical applications of a formalism for geophysical inverse problems. Geophys. J. R. astr. Soc., v. 92, p. 125-142.

Benz, H.M. and Smith, R.B. (1984) Simultaneous inversion for lateral velocity variation and hypocenters in the Yellowstone region using earthquakes and refraction data. J. geophys. Res., v. 89, p. 1208-1222.

Cho, J.D., Lim, M.T. and Park, I.H. (1997) The study on the Bouguer gravity anomaly of the Southern part of Korea. Bull. Seis. Asso. Far. East. (SAFE), v. 3, p. 212-224.

Crosson, R.D. (1976) Crustal structure modeling of earthquake data, 1. Simultaneous least square estimation of hypocenters and velocity parameters. J. geophys. Res., v. 81, p. 3036-3046.

Hawley, B.W., Zandt, G. and Smith, R.B. (1981) Simultaneous inversion for hypocenters and lateral velocity variations: an iterative solution with a layered model. J. geophys. Res., v. 86, p. 7073-7086.

Kim, O.J. (1987) Geology of Korea. Kyohak-Sa Publishing, Seoul.

Kim, S.G. and Gao, F. (1995) Korean Earthquake Catalogue. The Seismological Institute, Hanyang University. Ansan.

Kim, S.G. and Gao, F. (1997) Study on some characteristics of earthquakes and explosions using the polarization method. J. Phys. Earth, v. 45, p. 39-54.

Kim, S.J. and Kim, S.G. (1983) A study on the crustal structure of south Korea by using seismic waves. J. Korean Inst. Mining Geol., v. 16, p. 51-61.

Kim, S.K and Jung, B.H. (1985) The crustal structure of the southern part of Korea. J. Korean Inst. Mining Geol., v. 18, p. 151-157.

Kim, S.G. and Lee, S.K. (1994) Crustal modeling for the southern parts of the Korean Peninsula using observational data and ray method. Kor. Inst. Min. and Energy Res., v. 31, p. 549-558.

Koch, M. (1985a) A theoretical and numerical study on the determination of the 3-D structure of the lithosphere by linear and non-linear inversion of teleseismic traveltimes. Geophys. J. R. astr. Soc., v. 80, p. 73-93.

Koch, M. (1985b) Non-linear inversion of local seismic travel times for the simultaneous determination of 3D velocity structure and hypocenters-application to the seismic zone Vrancea. J. Geophys, v. 56, p. 160-173.

Koch, M. (1993) Simultaneous inversion for 3-D crustal structure and hypocentres including direct, refracted and reflected phase-I. Development validation and optimal regularization of the method., II. Application to the northern Rhine Graben/Rhenish Massif Region, Germany, III. Applicationto the southern Rhine Graben seismic region, Germany. Geophys. J. Int., v. 112, p. 385-447.

Lee, S.K. (1997) Study on the Crustal Structure of the Korean Peninsula Using Receiver Functions and Seismic Tomography. Ph.D. thesis, The Seismological Institute of Hanyang University, 248p.

Lees, L.M. and Crosson, R.S. (1989) Tomographic inversion for three-dimensional velocity structure at Mount St. Helens using earthquakes data. J. geophys. Res, v. 94. p. 5716-5728.

Li, Q. (1994) The 3-D seismic velocity structure in the northern segment of the North-South Seismic Zone. in Changma earthquake and research of M7 earthquakes. Seismological Press. Beijing.

Li, Q. Yuansheng, Z., Guoying, S. and Bing, F. (1994). The 3-D

seismic velocity structure in Hexi-Corrido, China., in Basic research on the dangeous area in the middle segment of Qilianshan Mountain. Seismological Press, Beijing.

Liu, F. (1984) Simultaneous inversion of earthquake hypocenters and velocity structure (I)-theory and method. Acta. Geophys. Sini. v. 27, p. 167-175.

Sambridge, M.S. (1990) Non-linear arrival time inversion: constraining velocity anomalies by seeking smooth models in 3-D. Geophys. J. Int., v. 102, p. 633-667.

Tarantola, A. (1987) Inverse problem theory, methods for data fitting and model parameter estimation. Elsevier, Amsterdam, New York.

Tarantola, A. and Valette, B. (1982) Generalized nonlinear inverse problems solved using the least square criterion. Rev. Geophys. Space Phys., v. 20, p. 219-232.

Thomson, C.I. and Gubbins, D. (1982) Three-dimensional lithospheric modeling at NORSAR: linearity of the method and amplitude variations from anomalies. Geophys. J.R. astr. Soc., v. 71, p. 1-36.

Thurber, C.H. (1983) Earthquake locations and three-dimensional structure in the Coyote Lake area, Central California. J. geophys. Res., v. 88, p. 8226-8236.

Thurber, C.H. (1985) Nonlinear earthquake location theory and examples. Bull. seismo. Soc. Am., v. 75, p. 779-790.

Walck, M.C. and Clayton, R.W. (1987) P-wave velocity variations in the Coso-region, California, derived from local earthquake travel times. J. geophys. Res., v. 92, p. 393-405.

Manuscript received 20 January, 1998

한반도 남부지역의 3-D 속도 토모그래피

金昭九 · 李清河

요 약 : 직접, 반사, 굴절파에 의한 3차원 속도구조를 위한 동시역산기술을 포함, 경상분지, 영남육괴 등 한반도 남부지역에 응용하였다. 44개 지진의 총 554개 지진 파선의 Pg, Sg, PmP, SmS, Pn, 그리고 Sn 위상의 주행시간은 진앙과 지각구조를 계산하기위해 사용하였다. 토모그래피 역산을 위해 수평으로는 0.5°의 grid로 이루어진 6×6 블록과 수직으로 4 km두께의 8개층으로 이루어진 불럭모델을 사용하였다. 3차원 속도 토모그래피 역산 결과 모호면에서 지표까지 8개층으로된 속도 깊이의 단면도를 작성하였으며, 수평속도분포는 위도와 경도별로 10개 수평속도분포도를 작성하였다. 그 결과는 다음과 같다. 1) 본 연구지역에서 퇴적암의 평균 속도는 5.04 km/sec, 두께는 3~4 km. 기반암의 평균속도는 6.11 km/sec임을 알았다. 그리고 천부층의 속도 변화는 남부지역을 대상으로 관측한 부우게 중력이상(Cho *et al.*, 1997)과 일치하는 것을 알았다. 2) 상부지각에의 수평 속도분포는 변화가 매우 크며 콘라드 밑의 하부지각의 수평 속도분포는 거의 일정함을 알았다. 3) 모호면의 평균깊이는 30.4 km, 평균속도는 8.01 km/sec 로 나타났다. 4) 퇴적층의 속도와 두께, 상부지각의 두께, 속도 그리고 모양, 모호면의 깊이와 모양 등에서 영남육괴, 경상분지, 그리고 포항분지의 차이를 명백히 찾을 수 있었다. 5) 경주, 포항지역 부근의 심부단층이 상부지각의 하부까지 연장된 정단층 또는 트러스트 단층임을 알았다.

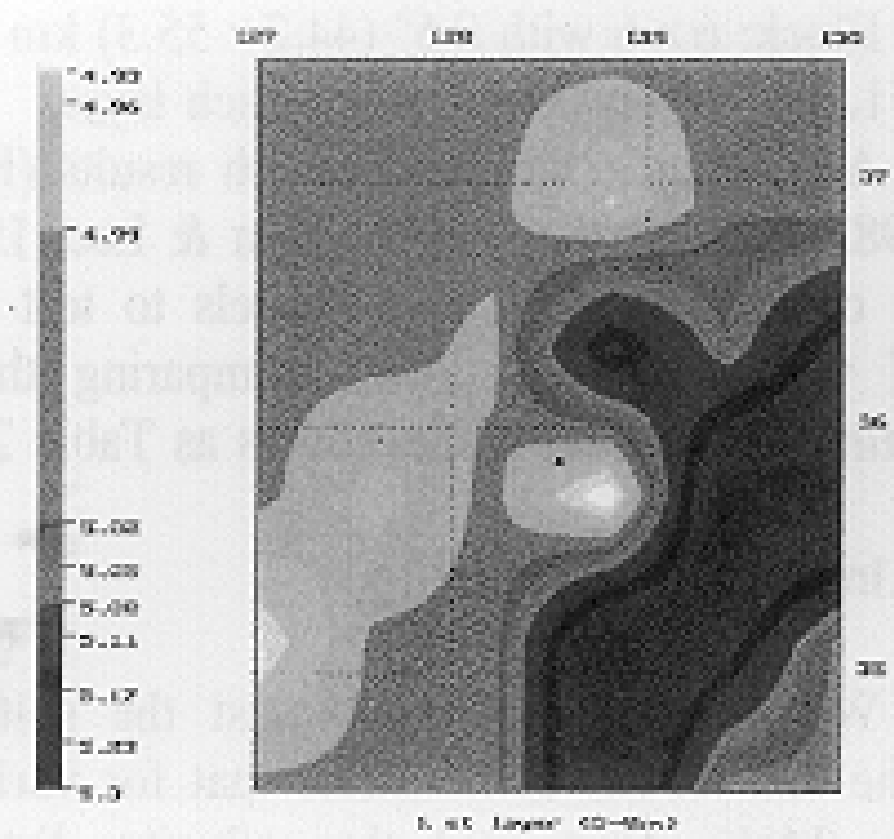

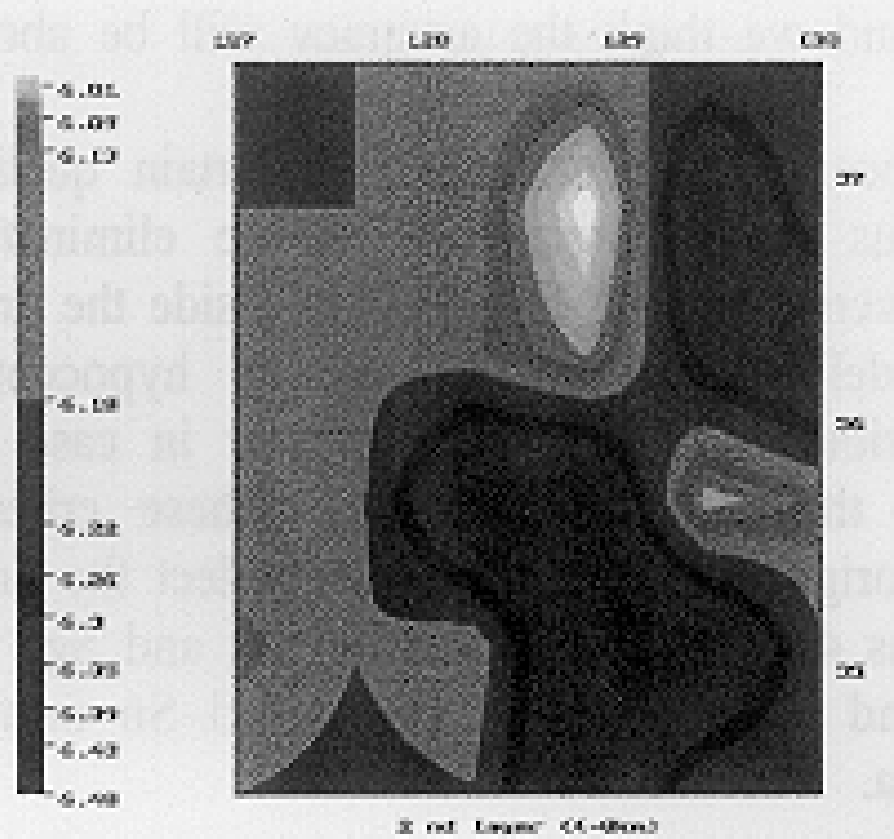

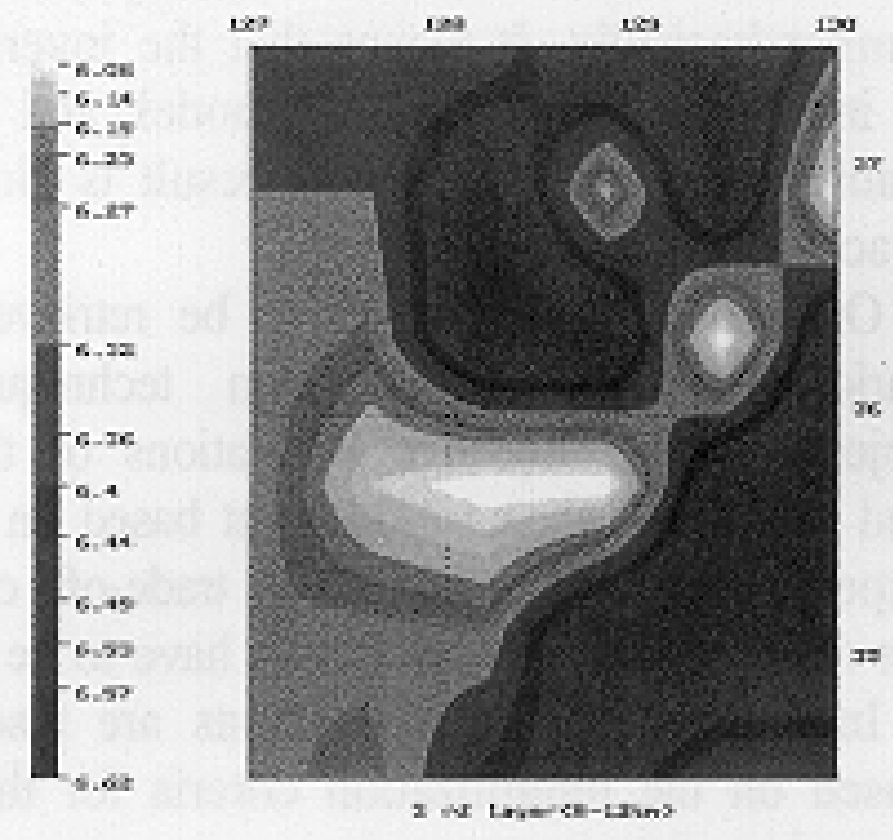

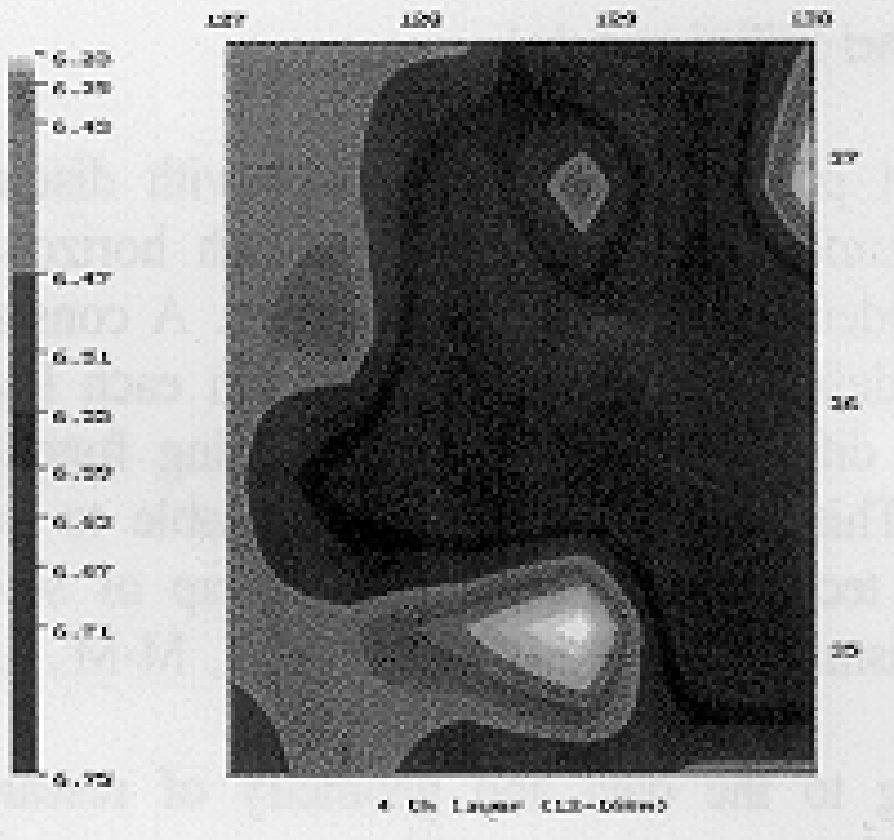

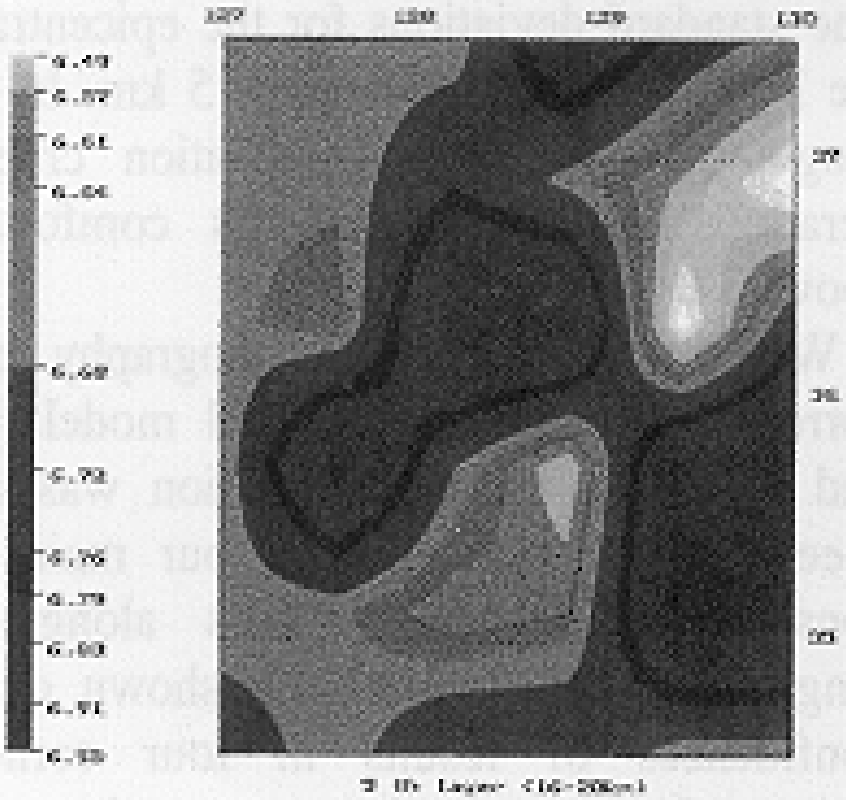
127
128
129
130
37
36
35

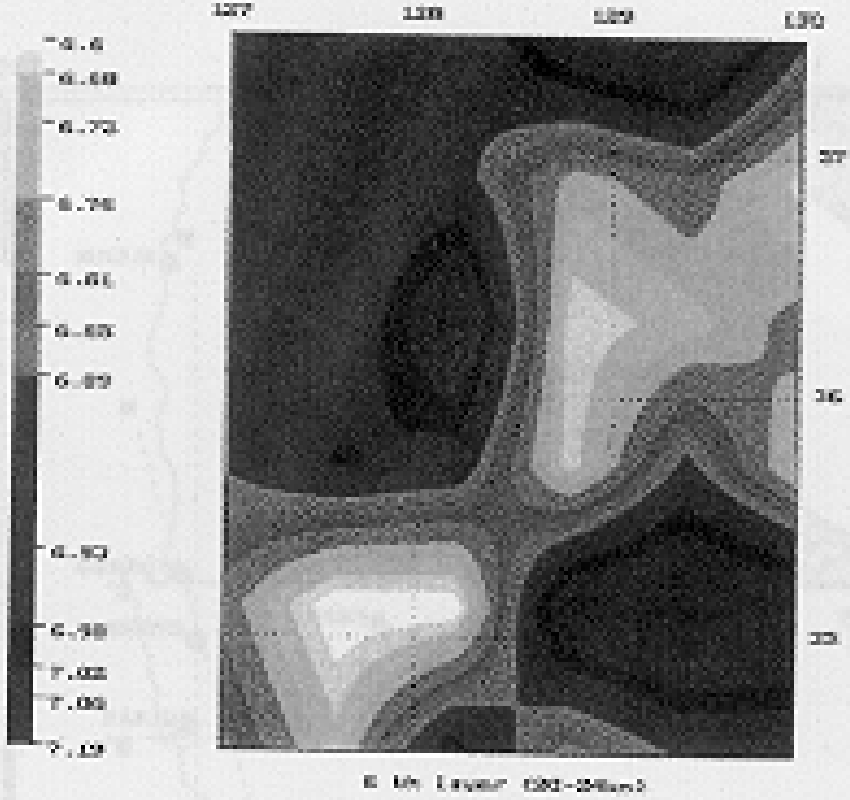
127
128
129
130
37
36
35

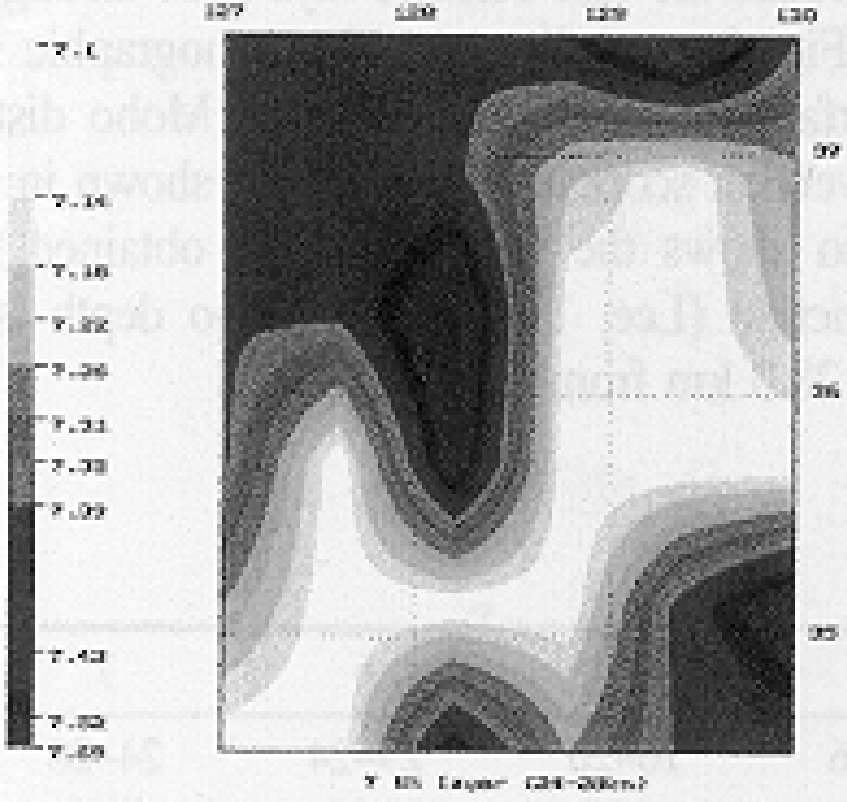
127
128
129
130
39
38
37

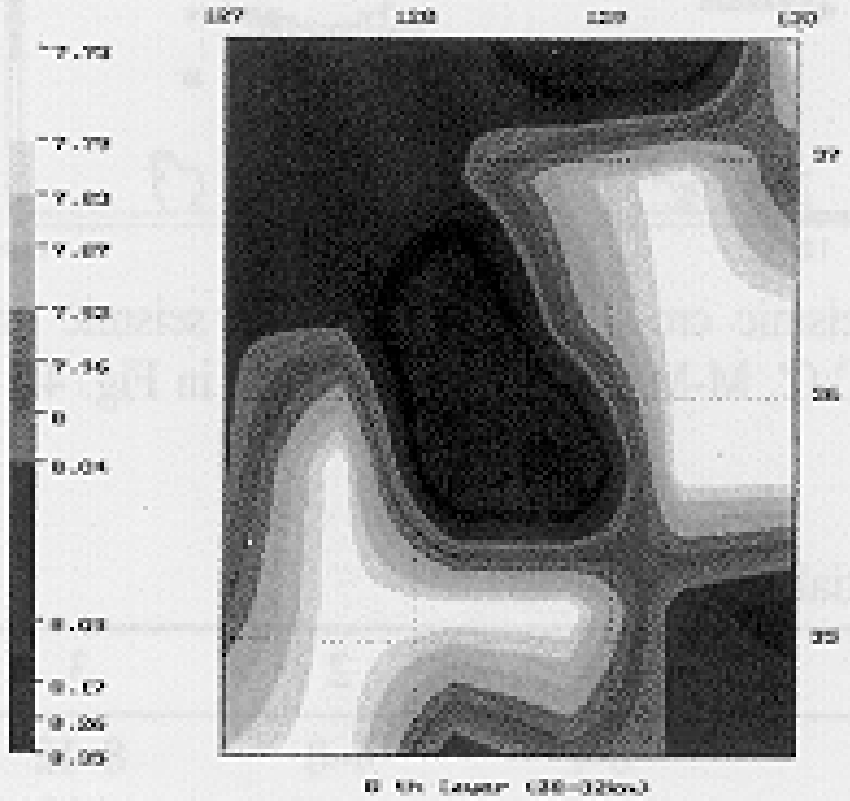
127
128
129
130
37
36
35

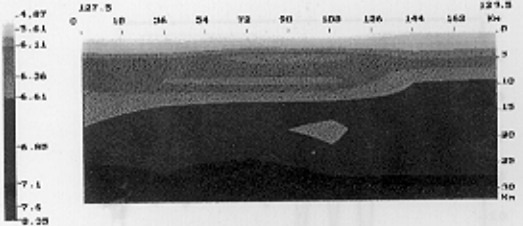
Profile C--C'

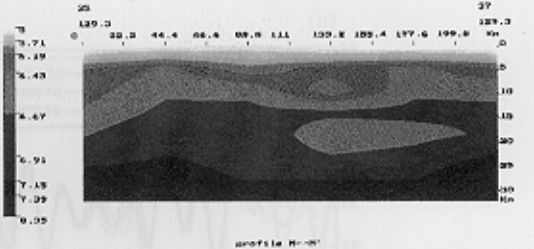
profile M--M'

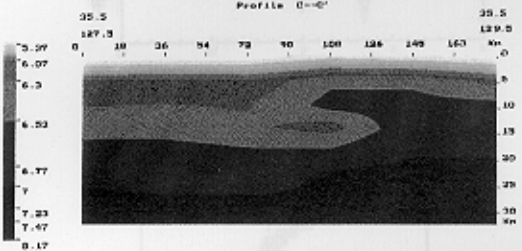
Profile B--B'

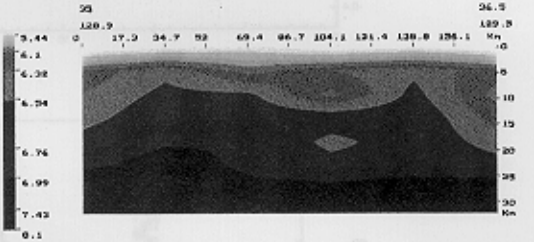
profile N--N'

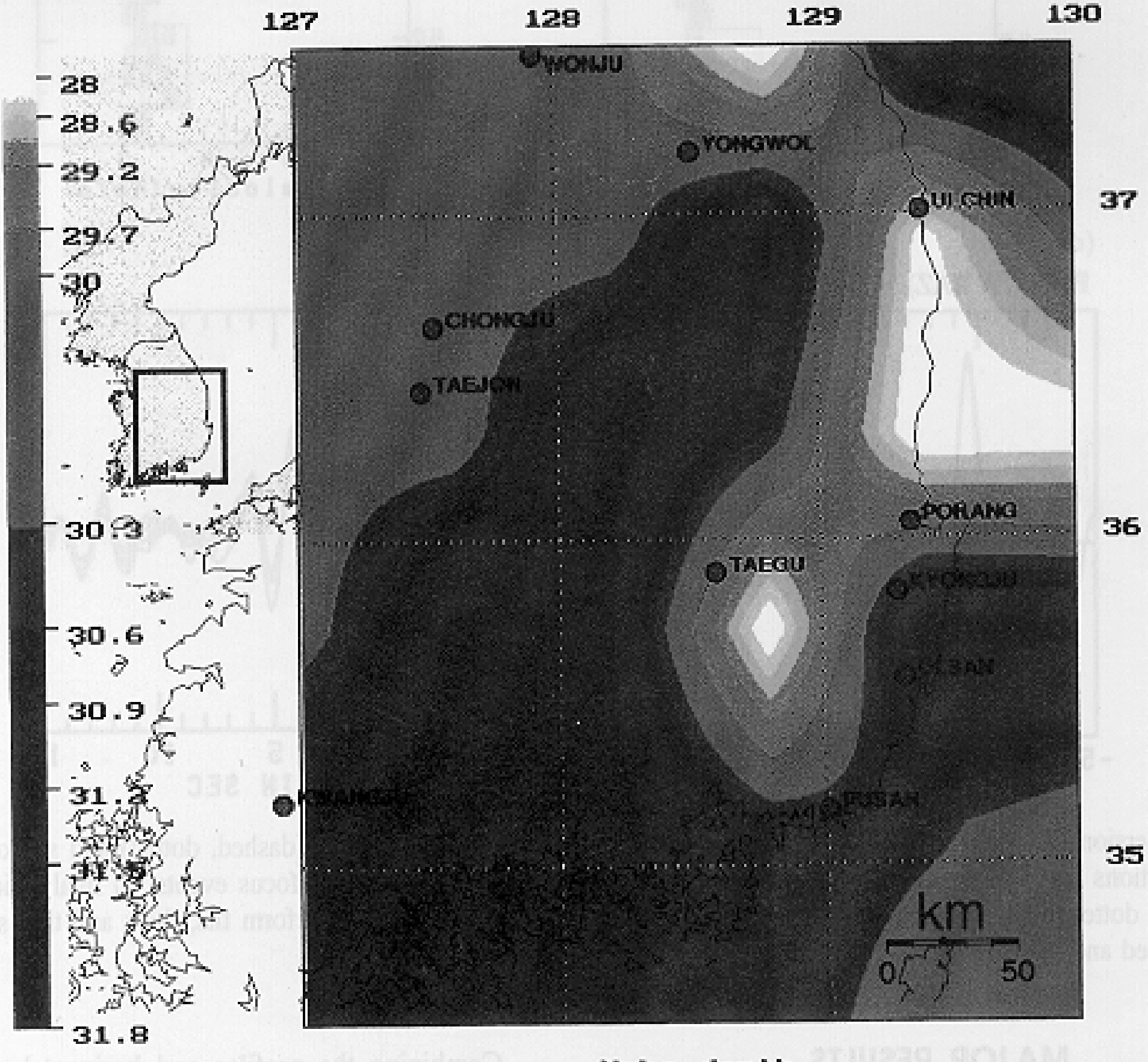
127
128
129
130
37
36
35
28
28.6
29.2
29.7
30
30.3
30.6
30.9
31.2
31.5
31.8
WONJU
YONGWOL
UI CHIN
CHONGJU
TAEJON
PORANG
TAEGU
KYONGJU
PUSAN
km
0
50

Moho depth